Magnetic and electromagnetic evaluation of the iron nanoparticle filled polyurethane nanocomposites

Zhanhu Guo, Sung Park, and H. Thomas Hahn

Mechanical & Aerospace Engineering Department and Materials Science & Engineering Department, University of California Los Angeles, Los Angeles, CA 90095

Suying Wei
Department of Chemistry, Louisiana State University, Baton Rouge, Louisiana 70803, USA

Monica Moldovan, Amar B. Karki, and David P. Young
Department of Physics and Astronomy, Louisiana State University, Baton Rouge, Louisiana 70803, USA

ABSTRACT

The magnetic and electromagnetic wave absorption behavior of a flexible iron-nanoparticle reinforced polyurethane nanocomposite is reported. Surface-initiated-polymerization (SIP) method was utilized to fabricate high quality nanocomposites with uniform particle distribution and tunable particle loading (up to 65 wt.%). The enhancement of coercive force is observed when the nanoparticles are embedded into the polymer matrix Electromagnetic wave absorption performance at a discrete frequency as studied by metal-backed reflection loss indicates that the SIP nanocomposites can save the weight up to 50% compared to the composite counterpart with micron-size particles.

Report Documentation Page

Form Approved
OMB No. 0704-0188

1. REPORT DATE	2. REPORT TYPE	3. DATES COVERED
01 MAY 2007	**N/A**	**-**

4. TITLE AND SUBTITLE	5a. CONTRACT NUMBER
Magnetic and electromagnetic evaluation of the iron nanoparticle filled polyurethane nanocomposites	5b. GRANT NUMBER
	5c. PROGRAM ELEMENT NUMBER
6. AUTHOR(S)	5d. PROJECT NUMBER
	5e. TASK NUMBER
	5f. WORK UNIT NUMBER
7. PERFORMING ORGANIZATION NAME(S) AND ADDRESS(ES) **Mechanical & Aerospace Engineering Department and Materials Science & Engineering Department, University of California Los Angeles, Los Angeles, CA 90095**	8. PERFORMING ORGANIZATION REPORT NUMBER
9. SPONSORING/MONITORING AGENCY NAME(S) AND ADDRESS(ES)	10. SPONSOR/MONITOR'S ACRONYM(S)
	11. SPONSOR/MONITOR'S REPORT NUMBER(S)

12. DISTRIBUTION/AVAILABILITY STATEMENT
Approved for public release, distribution unlimited

13. SUPPLEMENTARY NOTES

14. ABSTRACT

15. SUBJECT TERMS

16. SECURITY CLASSIFICATION OF:			17. LIMITATION OF ABSTRACT	18. NUMBER OF PAGES	19a. NAME OF RESPONSIBLE PERSON
a. REPORT	b. ABSTRACT	c. THIS PAGE			
unclassified	**unclassified**	**unclassified**	**UU**	**14**	

I. INTRODUCTION

Electromagnetic absorbers are a critical part of electronic systems in applications such as electromagnetic shielding for air vehicles and wireless communications.[1] However, the existing electromagnetic absorption materials have several drawbacks: heavy, less durable and effective only over fixed frequency bands. One way to improve the current electromagnetic absorbers is to exploit the polymer composites reinforced with magnetic nanoparticles (NPs). Magnetic nanoparticles could offer novel physicochemical properties arising from the core/shell structure and the particle interactions. Recent studies on magnetic nanocomposites show improvements in electromagnetic wave absorption by utilizing magnetic nanoparticles.[1-7] Another side benefit of using magnetic NPs as fillers that cannot be ignored is the nano-size scale in diameter. Since the metallic magnetic materials are conductive, the effective permeability decreases at high frequencies due to eddy current losses induced by electromagnetic waves.[8] However, the eddy current loss can be suppressed if the particle size is below the skin depth. At microwave frequencies (~10 GHz) of interest, the skin depth is typically around 1 μm,[9] and therefore nanoparticles will be fully effective throughout their volume in electromagnetic wave absorption. This paper reports on the magnetic and electromagnetic wave absorption properties of a highly particle-loaded magnetic nanocomposite fabricated by the surface-initiated-polymerization (SIP) method. The results are compared with the micron-metal-particle filled composites to evaluate the absorbing performance.

II. EXPERIMENTAL

The polyurethane (PU) composites reinforced with magnetic NPs having an iron core/iron oxide shell structure (average particle size of 20 nm, QuantumSphere Inc., CA)

were fabricated by the surface-initiated-polymerization (SIP) method. SIP was observed to fabricate a high particle loading of up to 65 wt.% in a polyurethane matrix while still maintaining the structural integrity.[10]

In the SIP method both the catalyst (a liquid containing aliphatic amine, parachlorobenzotrifluoride and methyl propyl ketone) and the accelerator (polyurethane STD-102, containing organo-titanate) were added into a nanoparticle suspended tetrahydrofuran solution. The two-part monomers (diisocyanate and diol, CAAPCOAT FP-002-55X, manufactured by the CAAP Co., Inc.) were then introduced into the above solution to polymerize for 6 h, and then poured into a mold for final curing. All the mixing steps were carried out with ultrasonication. Nanocomposites with 35 and 65 wt.% particle loadings were fabricated, respectively. For comparison purposes, carbonyl iron particles (CIP, BASF Group, 2-5 μm, 99.5 wt.% Fe) were also used to fabricate CIP-PU composites with a particle loading of 55, 70 and 79 wt.%, respectively. The densities of the composites were measured following the ASTM D792 standard.

Particle structural characterization was performed on a JEOL TEM-2010 transmission electron microscope (TEM). Weight percentage of NPs in the nanocomposites was determined by the thermogravimetric analysis (TGA, PerkinElmer) with an argon flow rate of 50 cm^{-3} min^{-1}. The magnetic properties were investigated in a 9-Tesla Physical Properties Measurement System (PPMS) by Quantum Design. The relative complex permeability and permitivity were measured using a transmission line technique. A washer-shaped specimen was cut from a thin sheet (~ 2 mm) of magnetic composite. The nominal outer and inner diameters of the specimen were 7.00 mm and 3.04 mm, respectively. The specimen was faced by abrading with a 320-grit SiC abrasive paper on a

granite flat until a smooth and uniform surface was achieved. The specimen was then placed in a sample holder, which was located in between the rigid beaded airline (APC-7) and the flexible coaxial airline (APC-7) that were connected to the network analyzer (HP Model 8510B). The frequency generator was used to generate electromagnetic waves from 2 to 18 GHz. The permeability and permitivity were then deduced from the scattering parameters using a Nicholson-Ross algorithm.[11] The metal backed reflection loss (MBRL) was calculated from the measured permitivity and permeability. The performance of the magnetic nanocomposites as a microwave absorber was thus evaluated and compared with the CIP-PU composites.

III. RESULTS AND DISCUSSION

Figure 1 shows the TEM bright field microstructures of the as-received Fe NPs. The obvious contrast within the particle in Figure 1 is due to the oxidation of the Fe nanoparticle. X-ray photoelectron spectroscopy (XPS) studies show that the iron oxide is Fe_2O_3 rather than other oxides (FeO and Fe_3O_4). The lattice distance of 0.2035 nm (ring 1), 0.1434 nm (ring 3), 0.1158 nm (ring 4), 0.1004 nm (ring 5), and 0.0827 nm (ring 6) of the selected area electron diffraction (SAED) in the inset of Figure 1 can be assigned to (110), (200), (211), (220) and (222) planes of Fe (Standard XRD file: PDF#06-0696 of iron); and 0.1673 nm (ring 2) arises from (430) plane of iron oxide (Standard XRD file: PDF#39-1346 of Fe_2O_3).

The particle distribution within the polyurethane matrix was characterized by a scanning electron microscope (SEM). The samples were prepared by embedding the flexible composite in a cured vinyl ester plug and polishing with 2000 grit sand paper. No

significant agglomeration was observed in the Fe-PU nanocomposite with a particle loading of 65 wt.%, as shown in the right inset of Figure 2. This indicates that the SIP method yields a high-quality nanocomposite.

Figure 2 shows the magnetic hysteresis loops of Fe-PU nanocomposites with different particle loadings. The saturation magnetization (M_s, 97.6 emu/g, based on the total mass) of the as-received nanoparticles is lower than that of the pure bulk iron (222 emu/g),[12] which is as expected because of the oxide shells. Little difference in M_s is observed for the nanoparticles embedded in the polyurethane matrix. The M_s is about 54 emu/g and 31.6 emu/g for the nanocomposites with a particle loading of 65 wt.% and 35 wt.%, respectively, which corresponds to 84 emu/g and 90.2 emu/g for the nanoparticles. The slightly lower M_s of the nanocomposites than that of the as-received NPs is attributed to the further oxidation of the NPs and the particle-polymer interfacial interaction.[13,14]

The low coercive force (coercivity, H_c; 5 Oe) indicates the superparamagnetic behavior of the as-received nanoparticles. The H_c of the polyurethane nanocomposites is 685 and 900 Oe for 65 and 35 wt.% loading, respectively, which are much larger than that of the as-received NP assembly. This trend is due to the interparticle dipolar interaction within the nanocomposite with a good dispersion of single-domain NPs, consistent with particle-loading-dependent coercivity in nanoparticle assembly.[15,16] Compared with the 35 wt.% nanocomposite, the smaller coercivity in the 65 wt.% nanocomposite arises from the decreased interparticle distance concomitant with a stronger dipolar interaction. However, the absence of H_c in the CIP and its composites is consistent with the characteristic of the micron-size soft particles, i.e., particle-loading-independent coercivity property.

Figures 3(a) and (b) show the relative permitivities (real and imaginary), and permeabilities (real and imaginary) of the CIP-PU composites and Fe-PU nanocomposites, respectively. The relative permitivities of the Fe-PU nanocomposites are higher than those of the CIP-PU composites, which is attributed to the existence of Fe particle chains as observed in the TEM image shown in Figure 1 and consistent with the composite system with metallic chain or flakes in a dielectric material which results in a high relative permitivity.[17] The real and imaginary permeabilities of the Fe-PU nanocomposites are lower than those of the CIP-PU composites, which is due to the larger magnetization of CIP particles (shown in Figure 2) compared to the Fe nanoparticles.

The metal-backed reflection loss coefficient (MBRL, dB) is given by Equation (1):

$$\text{MBRL[dB]} = 20\log_{10}\left|\frac{Z-1}{Z+1}\right| \qquad (1)$$

where Z is the relative impedance for a flat metallic surface coated with a dielectric layer given by Equation (2).

$$Z = \sqrt{\frac{\mu}{\varepsilon}}\tanh\left[-i2\pi\frac{d}{\lambda}\sqrt{\mu\varepsilon}\right] \qquad (2)$$

where μ and ε are the relative permeability and permitivity of the absorbing layer, respectively, d is the layer thickness, and λ is the wave-length in free space.[18]

In order to illustrate the relative performance of the nanocomposite, an absorber is designed to have the MBRL minimum of 20 dB at the target frequency of 10 GHz. Figure 4 shows the MBRL of the CIP-PU composite, Fe-PU nanocomposite and a commercially available microwave absorber (Q-Zorb Single Band Absorber with a thickness of 1.524 mm and density of 4.06 g/cc, RF Products, A Laird Technologies Company). The Q-Zorb

Single Band Absorber, a composite film made out of nitrile rubber reinforced with the micron-CIP, is resonantly tuned to develop a 20 dB loss at 10 GHz.

To develop the performance curves in Figure 4, the optimum thickness (based on the absorber requirement, i.e., having a minimum 20 dB MBRL at frequency of 10 GHz) of the CIP-PU composite film (79 wt.%, 3.153 g/cc) and the Fe-PU nanocomposite film (65 wt.%, 1.804 g/cc) was calculated to be 1.524 mm and 1.702 mm, respectively. When these thicknesses are combined with the densities, Fe-PU nanocomposite leads to weight savings of 37% and 50%, respectively, compared with the CIP-PU composite and the Q-Zorb Single Absorber. This suggests that the magnetic nanocomposite can be an excellent choice for the discrete frequency absorption applications. However, when the absorbed bandwidths are compared, the CIP-PU composite comes ahead of the Fe-PU nanocomposite film. The CIP-PU composite film shows a bandwidth of 7 GHz (7 ~ 14 GHz) while the Fe-PU nanocomposite film shows a bandwidth of only 2 GHz (9 ~ 11 GHz) for a reflection loss of 10 dB.

IV. CONCLUSION

The magnetic and microwave properties of the Fe-PU nanocomposite were evaluated and compared with those of the CIP-PU composite. Coercivity was found to be larger in the nanocomposite with lower particle loading and is negligible in the nanoparticle assembly, indicating the superparamagnetic behavior of these nanoparticles. Little coercivity is observed in the micron-size CIP and its composites. The calculated metal-backed reflection loss indicated that the Fe-PU nanocomposite can be used at a

substantial weight savings in a discrete frequency absorption application, when compared with the CIP-PU composite and the commercially available electromagnetic absorbers. These findings offer the feasibility of developing lighter-weight microwave absorbers by using magnetic nanocomposites. Magnetic nanoparticles with less iron oxide could improve the performance of nanocomposites with an increased bandwidth.

ACKNOWLEGEMENTS

This work was partially supported by the Air Force Office of Scientific Research through AFOSR Grant FA9550-05-1-0138 with Dr. B. Les Lee as the Program Manager. DPY kindly acknowledges support from the National Science Foundation under Grant No. DMR 04-49022. Appreciation is extended to QuantumSphere. Inc. for supplying the iron nanoparticles and for providing financial support for the TEM and XPS analyses.

REFERENCES

(1) V.B. Bregar, IEEE Trans. Magn. **40**, 1679 (2004**)**.

(2) J. R. Liu, M. Itoh, T. Horikawa, E. Taguchi, H. Mori, and K. Machida, Appl. Phys. A: Mater. Sci. Process. **82**, 509 (2006).

(3) C. Sudakar, G. N. Subbanna, and T. R. N. Kutty, J. Appl. Phys. **94**, 6030 (2003).

(4) T. Furubayashi, I. Nakatani, and N. Saegusa, J. Phys. Soc. Jpn. **56**, 1855 (1987).

(5) S. N. Khanna, and S. Linderoth, Phys. Rev. Lett. **67**, 742 (1991).

(6) F. Bodker, S. Morup, and S. Linderoth, Phys. Rev. Lett. **72**, 282 (1994).

(7) H. Ota, M. Kimura, R. Sato, K. Okayama, S. Kondo, and M. Homma, IEEE Symp. Electromagn. Compatibility, **2**, 590 (1999).

(8) M. Matsumoto, and Y. Miyata, IEEE Trans. Magn. **33**, 4459 (1997).

(9) S. Sugimoto, T. Maeda, D. Book, T. Kagotani, K. Inomata, M. Homma, H. Ota, Y. Houjou, and R.Sato, J. Alloy. Compd. **330-332**, 301 (2002).

(10) Z. Guo, S. Park, and H. T. Hahn, Nanocomposite fabrication through particle surface initiated polymerization, 2006 AICHE Annual Meeting, San Francisco, (2006).

(11) A. M. Nicolson, and G. F. Ross, IEEE Trans. Instrum. Meas., **IM-19**, 377 (1970).

(12) B. D. Cullity, Introduction to Magnetic Materials, Addison-Wiley, New York (1972).

(13) D. Zhang, K. J. Klabunde, C. M. Sorensen, and G. C. Hadjipanayis, Phys. Rev. B: Condens. Matter Mater. Phys. **58**, 14167 (1998).

(14) S. Gangopadhyay, G. C. Hadjipanayis, S. I. Shah, C. M. Sorensen, K. J. Klabunde, V. Papaefthymiou, and A. Kostikas, J. Appl. Phys. **70**, 5888 (1991).

(15) D. Kechrakos, and K. N. Trohidou, Phys. Rev. B, **58**, 12169 (1998).

(16) G. Xiao, and C. Chien, Appl. Phys. Lett. **51**, 1280 (1987).

(17) X. Zhang, T. Ekiert, K. M. Unruh, J. Q. Xiao, M. Golt, R. Wu, J. Appl. Phys. **99**, 08M914 (2006).

(18) E. F. Knott, J. F. Shaffer, and M. T. Tully, Radar Cross Section; 2 Edition, Sci.Tech. Publishing, New York, (2004).

Figure Captions

Figure 1. TEM bright field micrographs of as-received nanoparticles; inset shows the selected area electron diffraction pattern.

Figure 2. Hysteresis loops of nanocomposites with 35 wt.% and 65 wt.% particle loading and pure Fe particle; left inset shows the hysteresis of CIP-PU composite with 55 wt.%, 70 wt.% and 79 wt.% particle loading and pure CIP particles; right inset shows the SEM image of nanocomposite with 65 wt.% particle loading.

Figure 3. (a) Real permitivity ε' and imaginary permitivity ε", and (b) real permeability μ′ and imaginary permeability μ" of Fe-PU nanocomposite and CIP-PU composite (bold line represents the real and thin line represents the complex part).

Figure 4. Metal-backed reflection loss as a function of frequency for Fe-PU nanocomposite and CIP-PU composite.

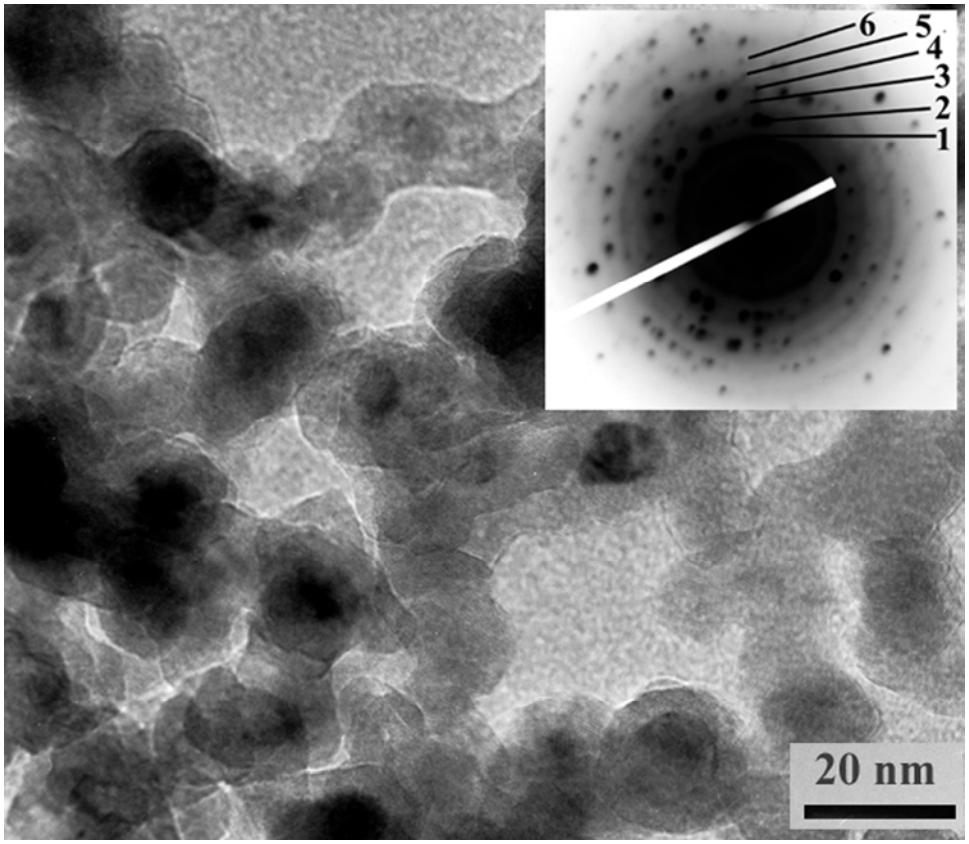

Figure 1. TEM bright field micrographs of as-received nanoparticles; inset shows the selected area electron diffraction pattern.

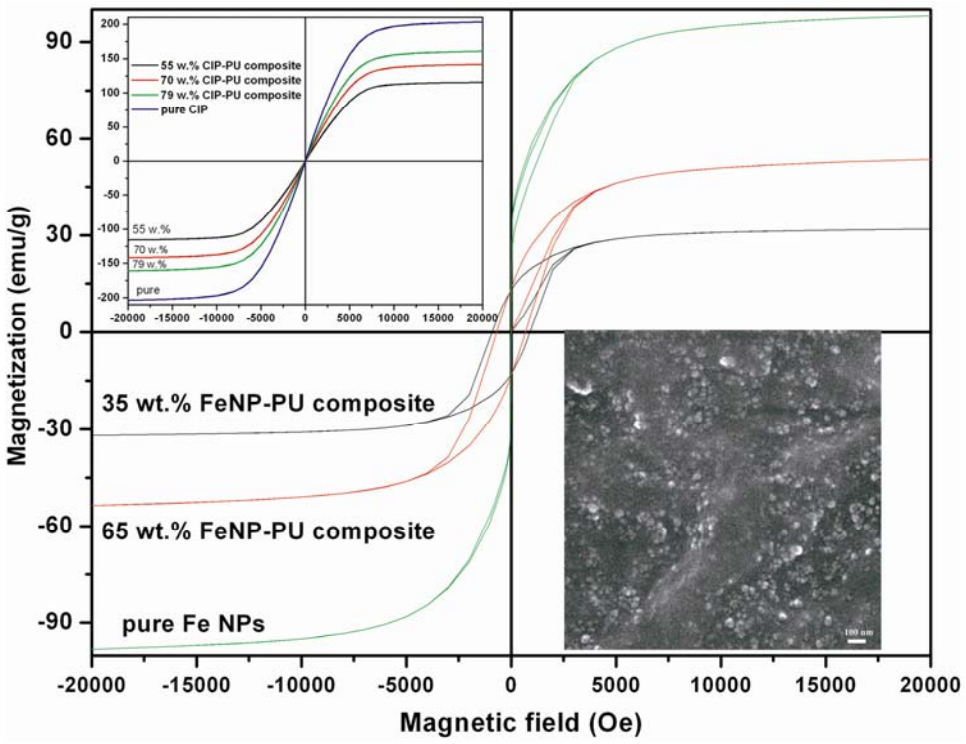

Figure 2. Hysteresis loops of nanocomposites with 35 wt.% and 65 wt.% particle loading and pure Fe particle; left inset shows the hysteresis of CIP-PU composite with 55 wt.%, 70 wt.% and 79 wt.% particle loading and pure CIP particles; right inset shows the SEM image of nanocomposite with 65 wt.% particle loading.

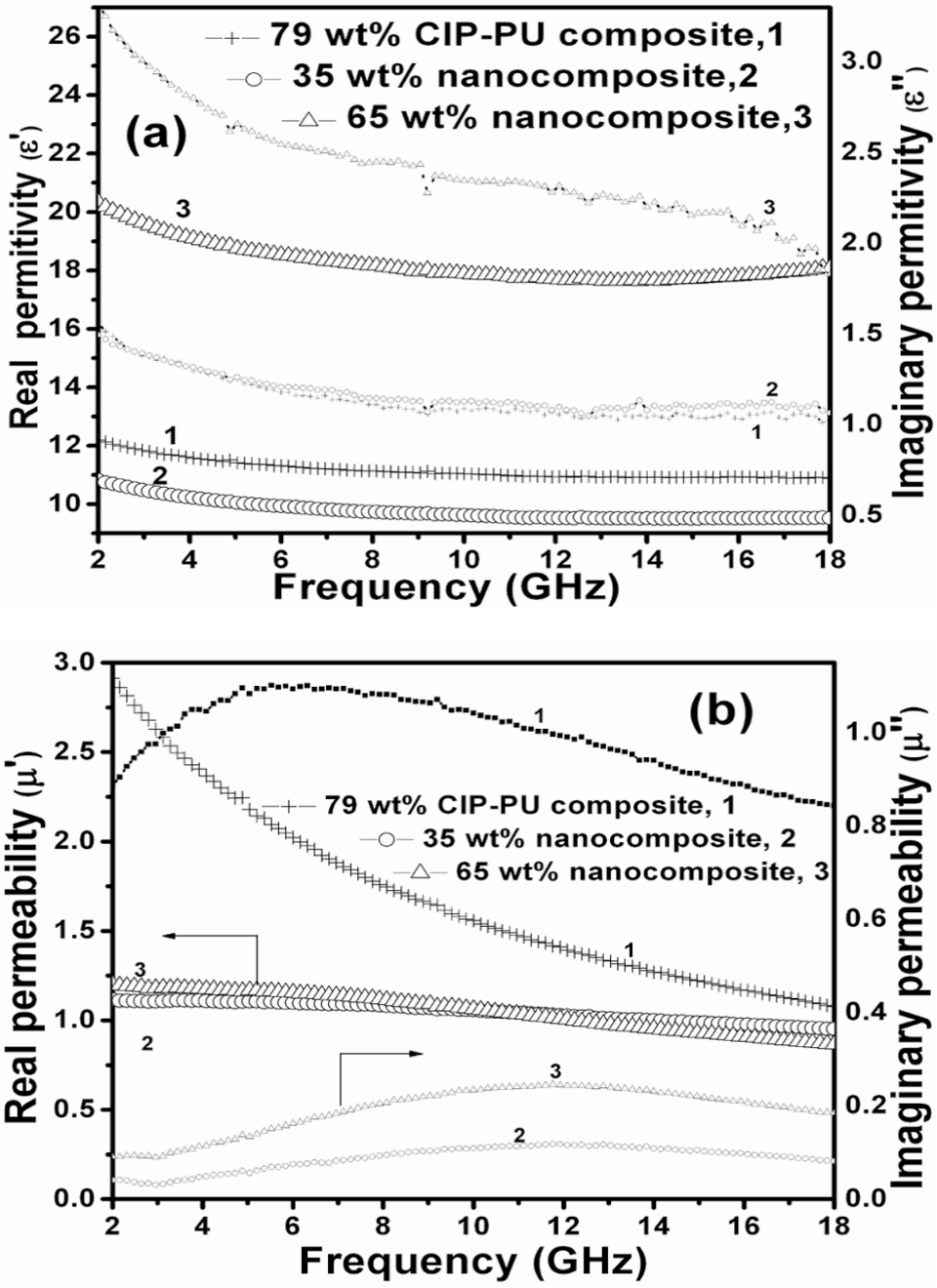

Figure 3. (a) Real permitivity ε' and imaginary permitivity ε", and (b) real permeability μ′ and imaginary permeability μ" of Fe-PU nanocomposite and CIP-PU composite (bold line represents the real and thin line represents the complex part).

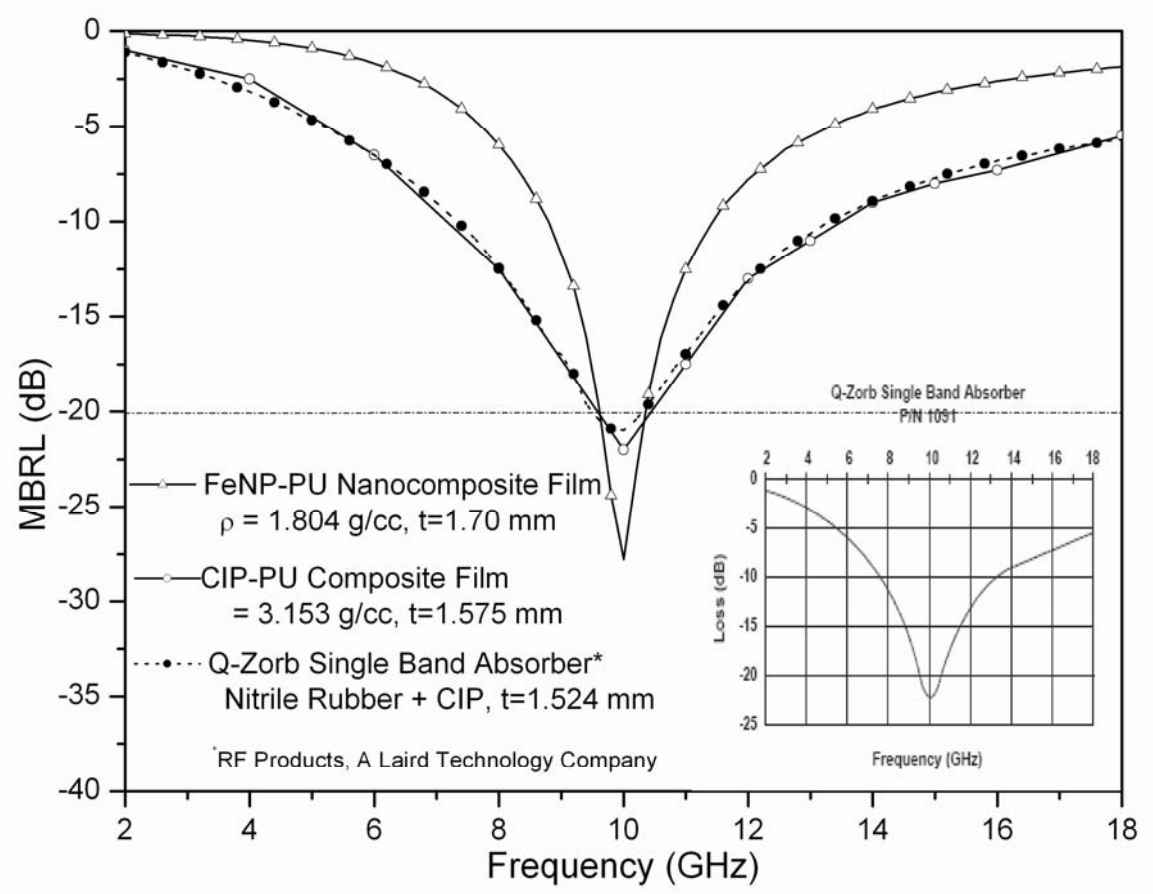

Figure 4. Metal-backed reflection loss as a function of frequency for Fe-PU nanocomposite and CIP-PU composite.